

Radiation-Sensitive Novel Polymeric Resist Materials: Iterative Synthesis and Their EUV Fragmentation Studies

V. S. V. Satyanarayana,[†] Felipe Kessler,[‡] Vikram Singh,[§] Francine R. Scheffer,[‡] Daniel E. Weibel,[‡] Subrata Ghosh,^{*,†} and Kenneth E. Gonsalves^{*,†,∇}

[†]School of Basic Sciences, Indian Institute of Technology Mandi, Mandi – 175001, Himachal Pradesh, India

[‡]Instituto de Química, Universidade Federal de Rio Grande do Sul, UFRGS, Avenida Bento Gonçalves 9500, P.O. Box 15003, 91501-970 Porto Alegre, RS, Brazil

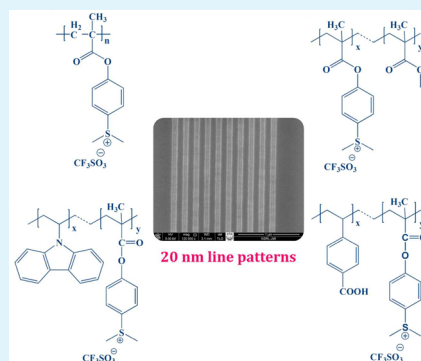
[§]School of Computing and Electrical Engineering, Indian Institute of Technology Mandi, Mandi – 175001, Himachal Pradesh, India

[∇]University of North Carolina, Charlotte, North Carolina 28223, United States

S Supporting Information

ABSTRACT: Polymerization of (4-(methacryloyloxy)phenyl)-dimethylsulfoniumtriflate (MAPDST), as a key monomer containing the radiation sensitive sulfonium functionality, with various other monomers such as methyl methacrylate (MMA), 4-carboxy styrene (STYCOOH), *N*-vinyl carbazole (NVK) in different molar ratios via free-radical polymerization method is described. This methodology led to the development of a small chemical library of six different radiation sensitive polymers for lithography applications. Fourier transform infrared (FT-IR) and nuclear magnetic resonance (NMR) spectroscopy identified the reaction products as MAPDST homopolymer and MAPDST-MMA, MAPDST-STYCOOH, MAPDST-NVK copolymers. Molecular weights were obtained from gel permeation chromatography and the decomposition temperature (T_d) values were determined using thermogravimetric analysis (TGA). The effect of extreme ultraviolet (EUV) irradiation on a thin poly(MAPDST) film was investigated using monochromatic synchrotron excitation. These new polymeric materials were also exposed to electron-beam lithography (EBL) and extreme ultraviolet lithography (EUVL) to achieve 20-nm line patterns.

KEYWORDS: radiation sensitive resist materials, characterization, EUV degradation, e-beam and EUV lithography



INTRODUCTION

The semiconductor industry has been promoting high-precision nanolithography to produce nanoscale transistors and integrated circuits (ICs) with enhanced density. Recently, next-generation lithography (NGL) technologies utilizing shorter wavelengths of light or a charged particle beam have been the subject of research to meet the resolution requirements of the Semiconductor Industry Roadmap (ITRS).¹ In conjunction with advances in the lithography tools, the development of novel resist materials is necessary as the resolution capability of conventional chemically amplified resists (CARs) have reached their limit at the 22-nm technology node. At features less than 20 nm, the lithographic line edge roughness (LER) and line width roughness (LWR) requirements become smaller than the size of polymer molecule and new resist designs are paramount. Upon examining the development of the microelectronics industry, it is evident that advanced organic materials have been necessary for realizing significant growth in semiconductors, storage, and display devices, because of the economies of scale. However, the maximum number of these organic polymers is used as photoresists (sacrificial stencils).

Photoresists are key materials that are designed to undergo a change in properties upon exposure to radiation and are extensively used to define chip circuitry.^{2–4} Specific photo-sensitive novel polymeric materials have been developed to meet requirements such as sensitivity, resolution, and processing needs of each successive chip generation.⁵

Organic polymeric materials have found many applications in optical and electronic devices.^{6–8} Many different organic monomers were polymerized to develop polymer systems for optical applications^{9–14} and interests have been focused on acrylic and methacrylic polymers, because of their well-known optical properties and good film-forming capability.^{15–17} A larger number of different methacrylic and acrylic monomers were prepared and polymerized previously under radical polymerization methods to produce distinct polymers with different functional groups, polarities by covering a broad range of molecular weights and glass-transition temperatures (T_g). At the same time, the multicomponent polymer systems containing various functionalities bonded to a methacrylate-

Received: December 21, 2013

Accepted: February 27, 2014

Published: February 27, 2014

based core have also been reported for their use in nanolithography.^{18–20}

In addition, polymers containing sulfonic acid groups in the form of salts have been studied intensively^{21,22} and used for both curing and microelectronic imaging of polymer films. Sulfonium groups have long been found to be sensitive to electron beam (e-beam) and ultraviolet (UV) radiation.^{23–26} Many polymers that were obtained from monomers in the form of sulfonium salts have been used as chemically amplified resists in lithography technology for high sensitivity and high resolution.^{27,28} However, these CARs have inherent limitations with respect to achieving features below 20 nm, as per the ITRS roadmap, because of acid diffusion, which contributes to image blur and leads to unacceptable LER and LWR, reduced resolution, and lower sensitivities. To overcome these drawbacks of current CARs, we have however utilized the radiation sensitivity of the sulfonium group to design novel negative tone nonchemically amplified resists (non-CARs).

Extreme ultraviolet lithography (EUVL) is one of the most promising exposure sources for NGL technology using the 13.5-nm EUV wavelength. Over the past decade, the development of EUV lithography has significantly progressed and approached its realization.²⁹ The development in the photoresist system greatly influences the achievable lithographic CD (critical dimension) as well as the quality of patterns transferred to the substrate through the mask. Recently, a variety of radiation-sensitive polymeric resist materials have been developed to satisfy several lithographic requirements such as low outgassing, high resolution, high sensitivity and reduction in line-edge roughness (LER)/line-width roughness (LWR).^{30–32} Nonetheless, significant improvements are still required.

Photons in the extreme ultraviolet (EUV) region to be used in NGL carry enough energy to break not only the chemical bonds of the polymers, but to produce ablation and a high yield of secondary electrons.^{29,33} An electron released as a result of photon absorption is also capable of breaking many molecular bonds of a polymer chain. As a result of the above high-energy processes outgassing, morphological and chemical changes in the polymer surface can lead to line edge roughness and pattern collapse, affecting resolution and cross-sectional profile. As a consequence, photons in the EUV region produce some unique challenges for EUV lithography that need to be investigated in detail with highly sensitive surface analytical techniques in high-vacuum environment.³⁴ This will assist in the progressive design of optimum resists for extreme ultraviolet lithography (EUVL).

Based on the above literature reports and in continuation of our work toward the non-CARs for e-beam or EUV lithography, herein we report the design, synthesis, and characterization of different novel organic polymeric resist materials based on the methyl methacrylate and sulfonium functionalities with high sensitivity, together with some preliminary EUV irradiation results of thin MAPDST homopolymer films. The microstructure of such advanced resists for EUVL and EBL is shown in Figure 1. The resists consist of essentially a radiation-sensitive sulfonium groups that, upon exposure, undergo a polarity change from hydrophilic to more-hydrophobic sulfides, as depicted in Figure 2. To enhance the sensitivity (photospeed) of these resists, various moieties can be incorporated in the microstructure, such as dissolution inhibitors and EUV absorption-enhancing units. The adhesion

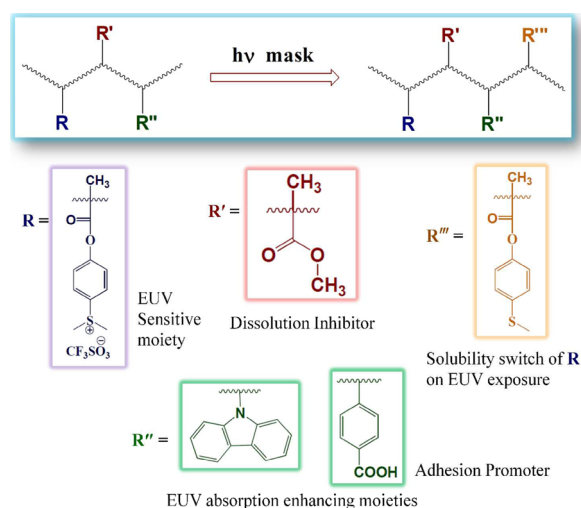


Figure 1. Polymer microstructures for advanced EUVL resist systems.

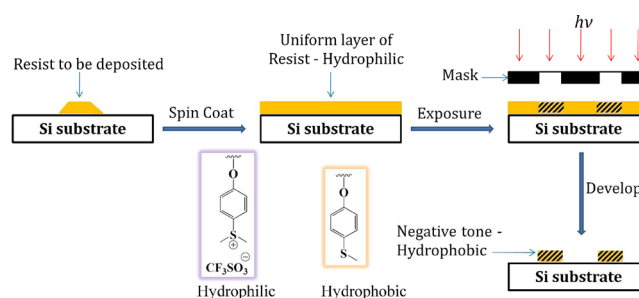


Figure 2. Schematic diagram of the lithographic process.

of resists to the silicon substrate can also be improved through the inclusion of adhesion promoters.

EXPERIMENTAL SECTION

Chemicals and Reagents. 4-Carboxy styrene (STYCOOH), *N*-vinyl carbazole (NVK) and *N,N*-diisopropylethyl amine (DIPEA) were purchased from Sigma–Aldrich and used as received. (4-Methyl mercapto)phenol, methacrylic acid (MAA), and tetramethylammonium hydroxide (TMAH) were purchased from Acros Organics. Methyl iodide, thionyl chloride (SOCl₂), and methyl methacrylate (MMA) were purchased from Loba Chemie. Tetrahydrofuran (THF) was dried using sodium wire/benzophenone, and acetonitrile (CH₃CN) was dried using calcium hydride (CaH₂). AIBN (Azobisisobutyronitrile) was purchased from Paras Polymers, India and recrystallized twice before use in polymerizations. Methacryloyl chloride (II), 4-(methylthio)phenyl methacrylate (III), and MAPDST [(4-(methacryloyloxy)phenyl)dimethylsulfonium triflate] monomer (IV) were prepared via the following reported literature procedures.^{35,36}

Procedure for the Synthesis of MAPDST Homopolymer (V). A 50-mL flask equipped with a magnetic stir bar was charged with 0.8 g (2.148 mmol) of MAPDST monomer, 1 wt % AIBN, and 12 mL of acetonitrile under a N₂ atmosphere. The mixture, after 1 h of N₂ purging, was left under magnetic stirring at 60 °C for 48 h under N₂ atmosphere. After completion, the reaction mixture was poured slowly into diethyl ether (50 mL) and the separated solid was washed with dichloromethane (DCM) and acetone. The resulting crude product was dissolved in methanol and then reprecipitated using diethyl ether. The separated white pure product was filtered and dried in a temperature-controlled hot-air oven at 50 °C for 1 day. Yield: 350 mg (43.75%). White solid. FT-IR: $\nu_{\max}/\text{cm}^{-1}$ 3025 and 2935 (CH), 1748 (C=O), 1639, 1588, and 1498 (aromatic C=C), 1254 (CF₃). ¹H NMR (500 MHz, DMSO-*d*₆) δ_{H} 8.13 (2H, br s, *m,m'*-ArH), 7.46 (2H,

Table 1. Polymerization Results of poly(MAPDST-co-MMA)

polymer	Feed Ratio (mol %)		Co-polymer Compositions ^a (mol %)		yield (%)	weight-average molecular weight, M_w^b (g/mol)	polydispersity index, PDI ^b	decomposition temperature, T_d^c (°C)
	MAPDST	MMA	MAPDST	MMA				
VIa	50	50	75	25	49.3	17700	2.45	189
VIb	83.3	16.7	90	10	71.5	8900	1.89	252
VIc	87.5	12.5	92	8.0	56.3	13700	2.47	219

^aCo-polymer compositions were calculated via ¹H NMR. ^b M_w and PDI were determined using PEO and PEG standards using DMF solvent. ^c T_d was measured at a heating rate of 10 °C/min in N₂.

br s, *o,o'*-ArH), 3.23 (6H, s, S(CH₃)₂), 2.34 (2H, br peak, CH₂ polymeric), 1.29 (3H, br peak, CH₃ aliphatic); ¹³C NMR (100 MHz, DMSO-*d*₆) δ_C 174.98 (C=O), 154.32, 132.14, 125.89, 124.44, 123.73, 122.76, 119.48, 117.63, 116.28 (aromatic, CF₃), 45.89 (CH₂), 28.81 (SCH₃), 19.91 (CH₃). ¹⁹F NMR (376 MHz; DMSO-*d*₆) δ_F -77.6 (3F, s, CF₃).

Procedure for the Synthesis of MAPDST-MMA Copolymer (VIa). MAPDST monomer (IV) (0.8 g, 2.148 mmol), methylmethacrylate (MMA) (0.215 g, 2.148 mmol), and AIBN (1% by weight, relative to both monomers) were dissolved under N₂ in a mixture of THF-CH₃CN (2:1) in a vial with a side arm and the resulting solution was siphoned to the polymerization flask equipped with a silicone septum and a Teflon stirring bar. The mixture, after 1 h of N₂ purging, was left under magnetic stirring at 60 °C for 48 h under N₂ atmosphere. After completion, the reaction mixture was poured slowly into diethyl ether (50 mL) and the separated solid was washed with dichloromethane (DCM). The resulting crude product was dissolved in methanol and then reprecipitated using diethyl ether. The separated white pure product was filtered and dried in a temperature-controlled hot-air oven at 50 °C for 1 day. Yield: 500 mg (49.3%). White solid. FT-IR: $\nu_{\max}/\text{cm}^{-1}$ 3031 and 2935 (CH), 1735 (C=O), 1639, 1588, and 1498 (aromatic C=C), 1254 (CF₃). ¹H NMR (500 MHz, DMSO-*d*₆) δ_H 8.10 (2H, br s, *m,m'*-ArH), 7.46 (2H, br s, *o,o'*-ArH), 3.54 (3H, split peak, OCH₃), 3.25 (6H, s, S(CH₃)₂), 1.95 (2H, br peak, CH₂ polymeric), 1.26 (3H, br peak, CH₃ aliphatic); ¹³C NMR (100 MHz, DMSO-*d*₆) δ_C 177.65, 176.99, 174.98 (C=O), 154.18, 132.34, 126.01, 124.63, 123.54, 122.71, 119.95, 116.38 (aromatic, CF₃), 52.53 (OCH₃), 45.92 and 44.55 (CH₂), 29.00 (SCH₃), 19.10 (CH₃). ¹⁹F NMR (376 MHz; DMSO-*d*₆) δ_F -77.6 (3F, s, CF₃).

MAPDST-MMA copolymers (VIb and VIc) were also prepared using the same procedure by changing feed ratios of monomers (see Table 1).

Procedure for the Synthesis of MAPDST-STYCOOH Copolymer (VIII). The same procedure for compound (VIa) was followed by using MAPDST monomer (IV) (0.9 g, 2.417 mmol), 4-carboxy styrene (STYCOOH) (VII) (0.1 g, 0.675 mmol), and AIBN (1% by weight, relative to both monomers), was left under magnetic stirring at 65 °C for 48 h under N₂ atmosphere. Yield: 690 mg (69.0%). White solid. FT-IR: $\nu_{\max}/\text{cm}^{-1}$ 3030 and 2935 (CH), 1753 (C=O), 1703 (COOH), 1636 and 1497 (aromatic C=C), 1263 (CF₃). ¹H NMR (500 MHz, DMSO-*d*₆) δ_H 6.96–8.08 (8H, br m, ArH), 3.25 (6H, s, S(CH₃)₂), 2.18 (3H, br peak, CH and CH₂ polymeric), 1.28 (3H, br peak, CH₃ aliphatic); ¹³C NMR (125 MHz, DMSO-*d*₆) δ_C 174.31 (C=O), 166.96 (C=O), 153.76, 131.53, 123.30, 121.96, 119.40, 116.84 (aromatic, CF₃), 64.97 (CH), 44.74 (CH₂), 28.46 (SCH₃), 18.63 (CH₃). ¹⁹F NMR (376 MHz; DMSO-*d*₆) δ_F -77.6 (3F, s, CF₃).

Procedure for the Synthesis of MAPDST-NVK Copolymer (X). The same procedure for compound (VIa) was followed by using MAPDST monomer (IV) (0.9 g, 2.417 mmol), *N*-vinyl carbazole (NVK) (IX) (0.1 g, 0.517 mmol), and AIBN (1% by weight, relative to both the monomers), was left under magnetic stirring at 65 °C for 48 h under N₂ atmosphere. Yield: 560 mg (56%). Off-white solid. FT-IR: $\nu_{\max}/\text{cm}^{-1}$ 3029 and 2934 (CH), 1750 (C=O), 1638 and 1587 (aromatic C=C), 1262 (CF₃). ¹H NMR (500 MHz, DMSO-*d*₆) δ_H 6.26–8.04 (12H, br m, ArH), 3.23 (6H, s, S(CH₃)₂), 2.15 (3H, br peak, CH and CH₂ polymeric), 1.22 (3H, br peak, CH₃ aliphatic); ¹³C

NMR (125 MHz, DMSO-*d*₆) δ_C 174.31 (C=O), 153.40, 131.79, 124.52, 123.30, 121.95, 119.39, 116.83 (aromatic, CF₃), 52.52 (CH), 44.72 (CH₂), 28.46 (SCH₃), 18.77 (CH₃). ¹⁹F NMR (376 MHz; DMSO-*d*₆) δ_F -77.6 (3F, s, CF₃).

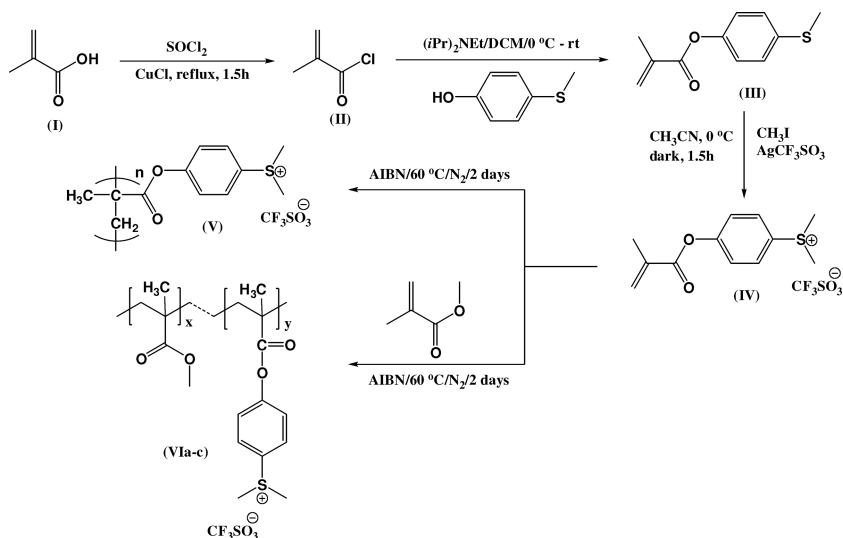
Characterization. Fourier transform infrared (FT-IR) spectra were recorded between 4000 cm⁻¹ to 400 cm⁻¹ using a Perkin-Elmer Spectrum 2 spectrophotometer at a resolution of 4 cm⁻¹ and averaging 16 scans per spectrum. ¹H and ¹³C NMR spectra were recorded on JEOL Model JNM ECX 500 MHz and 400 MHz spectrometers in deuterated dimethyl sulfoxide (DMSO-*d*₆) and methanol (MeOH-*d*₄) as solvents at ambient temperature. Molecular weights and polydispersity (PDI) were determined by performing gel permeation chromatography (GPC) analysis with PL gel mixed B and C 10- μ m columns, using an Agilent Technologies 1260 Infinity Series instrument. DMF with 0.1% LiBr was used as a mobile phase at a flow rate of 0.5 mL/min and a column temperature of 70 °C. Thermogravimetric analysis (TGA) measurements were done on Netzsch Model STA 449 F1 JUPITER Series instrument. The heating rate was 10 °C/min in N₂ atmosphere over a temperature range from 20 °C to 500 °C.

Imaging Experiment. Resist Processing. Resist solutions were prepared using 3% by weight of polymer in methanol by subsequent filtration through a 0.2 μ m Teflon filter and were used in all experiments. The substrates were 2-in.-diameter *p*-type Si (100) wafers purchased from Wafer World, Inc. Prior to spinning, silicon wafers were cleaned using an RCA cleaning method to remove organic contaminants, subjected to a dehydration bake at 200 °C for 10 min, and finally cooled to room temperature. The soft-bake was done on a hot plate to dry out the solvent completely. Resist-coated films were exposed at a beam energy of 20 keV with a 20- μ m aperture, and the beam current was 196.8 pA by covering a broad range of doses (see Supporting Information for details). For EUV exposure evaluation, resist solutions were spin-coated on HMDS-treated 200 mm silicon wafers for ~40 nm thin films, followed by a soft-bake, and the resultant thin films of photoresists were flood-exposed with the respective E₀ array using SEMATECH Berkeley Microfield Exposure Tool (MET), which is a high-resolution EUV (13.5 nm) lithography tool. Samples were exposed using mask IMO228775 with a field of R4C3. A post-exposure bake (PEB) method was followed, to obtain good resist mask edges using a hot plate. Development was completed using standard concentration TMAH, 0.003 N aqueous solution by maintaining pH 11.5 at room temperature, rinsed with DI water, and finally dried by passing pure nitrogen gas over the films (see the Supporting Information for details).

Imaging. Resolution and image quality were determined by examining the developed resist profiles with SEM attached to Raith 150 lithography system at INUP, IIT Bombay. The exposed features were evaluated at energy of 5 keV. HRSEM images were taken using Nova Nano SEM 450 FEI instrument HRSEM at JMI Central University (New Delhi, India).

Thin Film Irradiation and Characterization. Thin MAPDST homopolymer films (~100 nm thickness) were prepared inside a glovebox in a dry and inert atmosphere by the spin-coating technique from a ~10⁻⁴ mol/L chloroform solution. The films were cast on ~5 × 10 mm Si (100) wafers. Oxygen (99.99%, White Martins-Praxair, Inc.) was used as received.

Scheme 1. Synthesis of MAPDST Homopolymer and MAPDST-MMA Co-polymer



Synchrotron radiation (SR) experiments were carried out at the Brazilian Synchrotron Light Source (LNLS), Campinas, Brazil. The Planar Grating Monochromator (PGM) beamline, for VUV and soft X-ray spectroscopy (100–1500 eV), which gives a spectral resolution ($E/\Delta E$) of 25 000, was used as the monochromatic photon source. The experimental setup includes a XYZ sample manipulator housed in an ultrahigh vacuum (UHV) chamber with a base pressure of 10^{-7} Pa. The silicon wafers were directly attached to the sample holder by using conducting double-sided tape and the SR beam was slightly defocused. No sample charging was observed throughout the experiments.

X-ray photoelectron spectroscopy (XPS) data were obtained using a high performance hemispheric SPECSLAB II (Phoibos-Hs 3500 150 analyzer, SPECS) energy analyzer. A pass energy of 50 eV was used for the survey spectra, whereas high-resolution (HR)-XPS spectra of single core atom excitations were recorded with a pass energy of 10 eV. The C 1s signal (position of the C–C/C–H signals), 285 eV, was used for energy calibration. The HR-XPS envelopes were analyzed and peak-fitted after subtraction of the Shirley background, using Gaussian–Lorentzian peak shapes obtained from the CasaXPS software package.

Near-edge X-ray absorption fine structure (NEXAFS) spectra were obtained by measuring the total electron yield (electron current at the sample) simultaneously with a photon flux monitor (gold grid). The final data were normalized by this flux spectrum to correct for fluctuations in beam intensity.

When SR was used to irradiate the films, a specific energy was selected (103.5 eV) that corresponds to the maximum intensity of ondulatory radiation at the PGM beamline. During selected fixed periods of time the polymer was irradiated under UHV conditions. After irradiation, pure oxygen at atmospheric pressure was introduced into the UHV chamber for 30 min to neutralize the remaining radicals on the film surface. Finally, XPS and NEXAFS spectra were obtained before and after irradiation. In addition, a quadrupole mass spectrometer (QMS) was integrated into the vacuum chamber in order to examine the volatile defragmentation products ablated from the irradiated polymer surface by an in situ gas analysis.

RESULTS AND DISCUSSION

A series of organic polymers, based on (4-(methacryloyloxy)-phenyl)dimethylsulfonium triflate (MAPDST) or on a combination of MAPDST and methylmethacrylate (MMA) or 4-carboxy styrene (STYCOOH) or N-vinyl carbazole (NVK) to increase the sensitivity toward e-beam or EUV, were prepared (see Schemes 1–3). MAPDST monomer is the crucial part in designing a polymer containing sulfonium

functionality at the para position of phenyl ring for the preparation of nonchemically amplified polymeric resist materials. MAPDST monomer (IV) was synthesized by reacting 4-(methylthio)phenylmethacrylate (III) with silver trifluoromethanesulfonate and iodomethane in acetonitrile at 0 °C in darkness under a N_2 atmosphere. Compound III was synthesized from the reaction between 4-(methylmercapto)phenol and methacryloyl chloride (II) in the presence of N,N' -diisopropylethylamine using dichloromethane solvent at 0 °C under a N_2 atmosphere (Scheme 1; see the Supporting Information for the detailed reaction procedures).

Homopolymerization of MAPDST monomer was initiated by 1 wt % AIBN in acetonitrile at a temperature of 60 °C under a N_2 atmosphere for 2 days. MAPDST homopolymer was obtained as a white powder with 40% yield. GPC measurement showed a weight-average molecular weight (M_w) of 20.7×10^3 g/mol, with a polydispersity index (PDI) of 2.52 for this polymer.

MAPDST-MMA co-polymers were prepared by using different molar ratios of MAPDST and MMA monomers (see Table 1). Polymerizations were carried out by free radical polymerization method using AIBN (1% by weight, relative to both monomers) as an initiator in a combined organic solvent of tetrahydrofuran (THF) and CH_3CN (2:1 ratio) at 60 °C under a N_2 atmosphere for 2 days. The compositions of co-polymers were calculated using 1H NMR and are given in Table 1. The molecular weights of the synthesized co-polymers were determined using gel permeation chromatography (GPC), and the weight-average molecular weight ranged from $M_w = 8900$ to $M_w = 17\,700$ (see Table 1).

Both FT-IR and NMR confirmed the chemical structures of the MAPDST homopolymer and MAPDST-MMA/STY-COOH/NVK copolymers. The 1H NMR spectra of MAPDST monomer (IV), homopolymer (V), and MAPDST-MMA copolymer (VIa) are shown in Figure 3. The resonance peaks of all the protons of homo and copolymers are readily assignable. The resonance of olefinic protons of MAPDST monomer are located at δ 5.95 and 6.32, which almost disappeared in the spectrum of homopolymer (V) and copolymer (VIa). This confirms the complete conversion of monomer into polymers (see the Supporting Information for details).

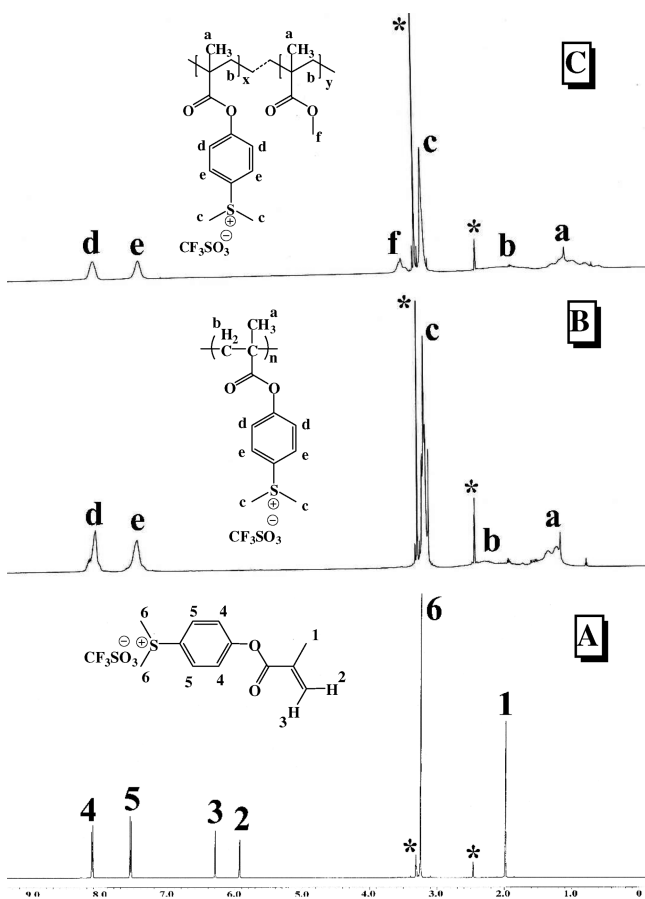


Figure 3. ¹H NMR spectra of (A) monomer (IV), (B) homopolymer (V), and (C) copolymer (VIa).

IR spectra of MAPDST homo and co-polymers exhibiting absorption bands at 1748, 1735, and 1254 cm^{-1} indicate the presence of C=O stretching and CF_3 stretching, respectively, and ¹³C NMR spectra of homo (V) and copolymer (VIa) show signals δ 174.98 and 177.65, 176.99, 174.98 indicating the presence C=O carbon, respectively. The carbon resonance peak of methoxy group (OCH_3) of methacrylate moiety at δ 52.53 indicates the formation of co-polymer (VIa).

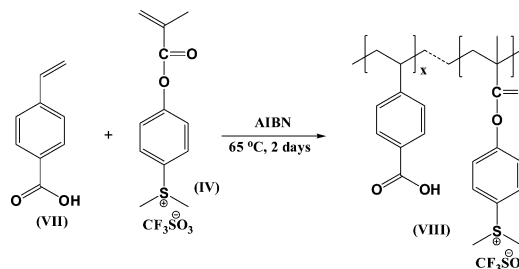
The FT-IR and NMR (see the Supporting Information for details) spectral profiles of VIb and VIc are similar to that of VIa. These results confirm the structure of MAPDST-MMA copolymers obtained from the free radical polymerization process.

Thermogravimetric analysis (TGA) was used to investigate the thermal stabilities of the polymers (Figure 5). TGA was performed at a heating rate of 10 $^{\circ}\text{C}/\text{min}$ under an N_2 atmosphere to measure the decomposition temperatures of the polymers. In TGA analyses, all these polymers exhibited distinct thermal transition peaks in the scanning range of 20–500 $^{\circ}\text{C}$. Table 1 summarizes the corresponding decomposition temperatures (T_d , 5% weight loss). The decomposition temperatures of MAPDST homopolymer (V) and MAPDST copolymers with MMA (VIa, VIb, and VIc) were 226 $^{\circ}\text{C}$ and 189, 252 $^{\circ}\text{C}$, 219 $^{\circ}\text{C}$, respectively, indicating suitable thermal stability for lithographic applications.

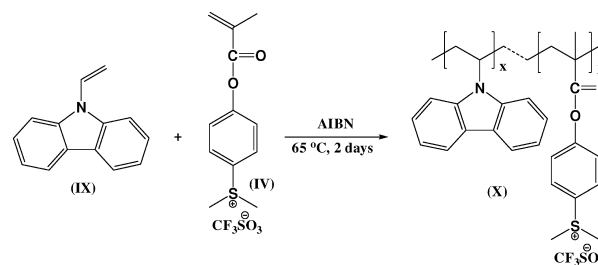
MAPDST-STYCOOH (VIII) and MAPDST-NVK (X) copolymers were prepared by similar free radical polymerization method using AIBN (1% by weight relative to both the monomers) as initiator in a combined organic solvent of

tetrahydrofuran (THF) and CH_3CN (2:1 ratio) at 65 $^{\circ}\text{C}$ under N_2 atmosphere for 2 days (see Schemes 2 and 3).

Scheme 2. Synthesis of Poly(MAPDST-co-STYCOOH)



Scheme 3. Synthesis of Poly(MAPDST-co-NVK)



The structures of MAPDST-STYCOOH and MAPDST-NVK copolymers were characterized using spectroscopic techniques. The ¹H NMR spectra of VIII and X are shown in Figure 4, and the resonance peaks for all the protons of copolymers (VIII and X) are readily assignable (see the Supporting Information for details).

The successful synthesis of MAPDST-STYCOOH and MAPDST-NVK co-polymers was also proved by FT-IR and ¹³C NMR measurements. For example, there are two characteristic absorption bands for the VIII co-polymer, at 1703 cm^{-1} and 1753 cm^{-1} , corresponding to C=O stretching vibrations of carboxylic and methacrylate functionalities, respectively. A strong absorption band at 1263 cm^{-1} is assigned for C–F stretching of CF_3SO_3 functionality. This clearly confirms the presence of MAPDST and 4-carboxy styrene moieties in the co-polymer structure, poly(MAPDST-co-STYCOOH). Infrared (IR) spectra of poly(MAPDST-co-NVK) exhibiting absorption bands at 1750 and 1262 cm^{-1} indicate the presence of C=O stretching of methacrylate moiety and CF_3 stretching of CF_3SO_3 functionality, respectively.

¹³C NMR spectra of MAPDST co-polymers (VIII and X) were recorded in $\text{DMSO}-d_6$. The carbon resonance of the carbonyl (C=O) and aromatic groups appear at a range of δ 174.31, 166.96, and 116.83–153.76 ppm; other chemical shifts belonging to polymeric CH/CH_2 carbons, CH_3 attached to a sulfonium moiety and CH_3 attached to a polymeric chain of copolymers VIII and X respectively appear at a range of δ 64.97/44.74 and 52.52/44.72, 28.46 and 18.63, and 18.77 ppm.

The molecular weights of the synthesized copolymers were determined using GPC, and the weight-average molecular weights of MAPDST-STYCOOH (VIII) and MAPDST-NVK (X) copolymers were $M_w = 2800$ and $M_w = 15\,200$ with a polydispersity (PDI) of 1.199 and 2.148, respectively (see Table 2). According to our previous reports, styrene-containing co-polymers show low molecular weights.^{19,27} The styrene-

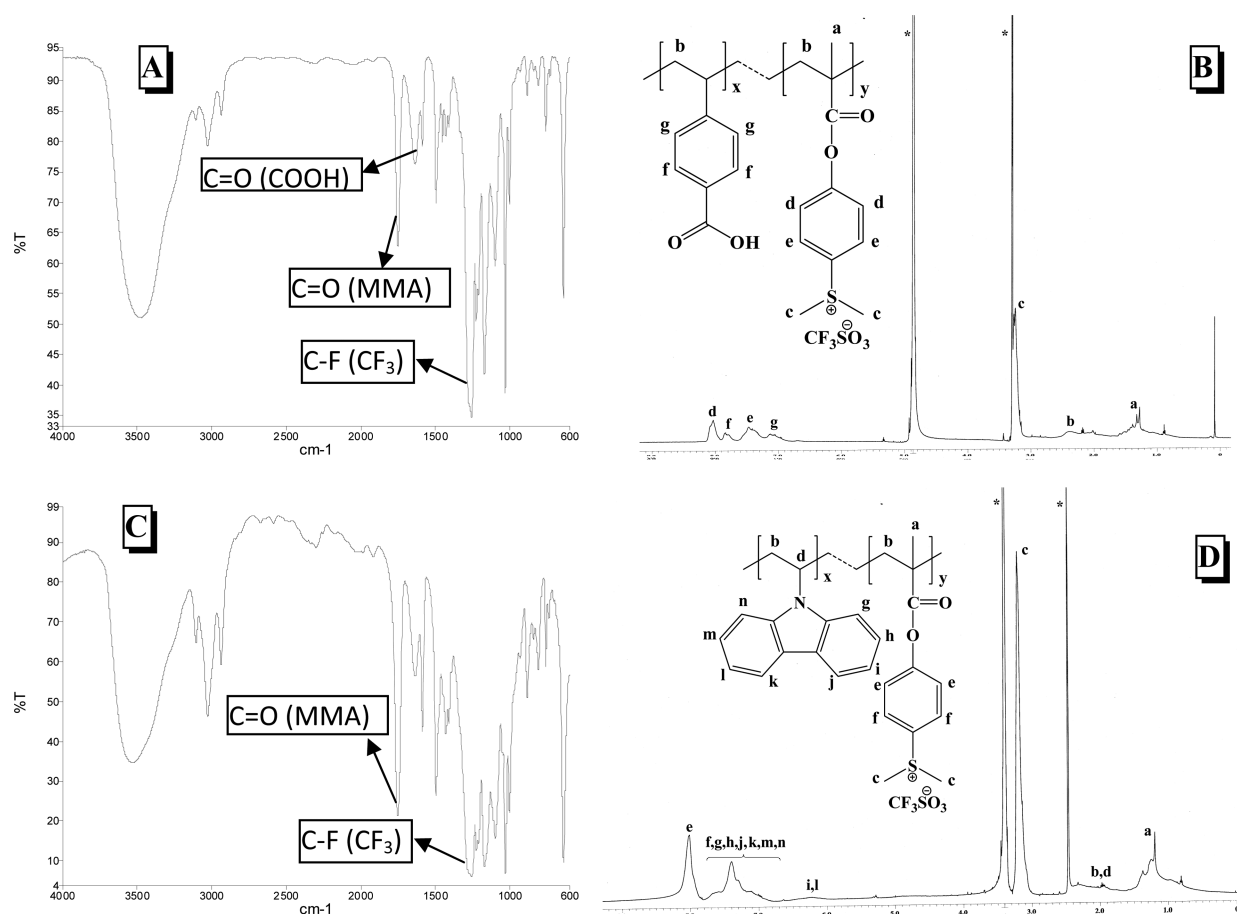


Figure 4. (A, C) FT-IR and (B, D) ^1H NMR spectra of poly(MAPDST-*co*-STYCOOH) (panels A and B) and poly(MAPDST-*co*-NVK) (panels C and D).

Table 2. Polymerization Results of Poly(MAPDST-*co*-STYCOOH) and Poly(MAPDST-*co*-NVK)

polymer	Feed Ratio (wt %)		Copolymer Compositions ^a (wt %)			yield (%)	weight-average molecular weight, M_w^b (g/mol)	polydispersity index, PDI ^b	decomposition temperature, T_d^c (°C)
	MAPDST	STYCOOH	NVK	MAPDST	STYCOOH				
VIII	90	10		84	16	69	2800	1.199	225
X	90		10	87		56	15200	2.148	148

^a Co -polymer compositions were calculated via ^1H NMR. ^b M_w and PDI were determined using PEO and PEG standards using DMF solvent. ^c T_d was measured at a heating rate of 10 °C/min in N_2 .

based co-polymer (VIII) was also found to have low molecular weight, compared to other newly developed polymers. Thermogravimetric analysis (TGA) was used to investigate the thermal stabilities of the polymers (Figure 5). Table 2 summarizes the corresponding decomposition temperatures (T_d , 5% weight loss). The decomposition temperatures of poly(MAPDST-*co*-STYCOOH) and poly(MAPDST-*co*-NVK) co-polymers were 225 and 148 °C, respectively, indicating good thermal stability and suitability for lithographic applications.

EUV Irradiation. To meet the resolution requirements for next-generation node technology, a value of 13.5 nm (98.5 eV) has emerged as a potential excitation energy.³⁷ Despite that information, there is a lack of detailed irradiation studies in this energy region, particularly with regard to chemical changes, outgassing, and new functional groups that are generated on the surface region after irradiation. The excitation energy of 103.5 eV is close to 98.5 eV and due to its high intensity in the PGM

beamline; it was selected to test the effect of the EUV radiation on the MAPDST homopolymer films.

XPS spectroscopy was used to prove the surface chemical changes after irradiation. Survey XPS spectra of pristine and irradiated MAPDST homopolymer films showed a continuous decrease in the F 1s and O 1s signal together with an increase in the C 1s signal with the increase in the irradiation time (see Supporting Information for details). The changes in the surface chemistry with the irradiation time can be seen clearly in the HR-XPS spectra of the C 1s envelope (Figure 6).

C 1s HR-XPS spectra revealed a clear change in the surface chemistry of the MAPDST homopolymer film after irradiation at 103.5 eV. The untreated films showed typical signals corresponding to the aliphatic and aromatic contributions (C–C/C–H), C–O, COO, and CF_3 functionalities. After 1 min of irradiation time, the CF_3 and COO contributions in the XPS spectra almost disappeared, whereas the C–O contribution was also strongly affected by the SR light. The CF_3 (from triflate)

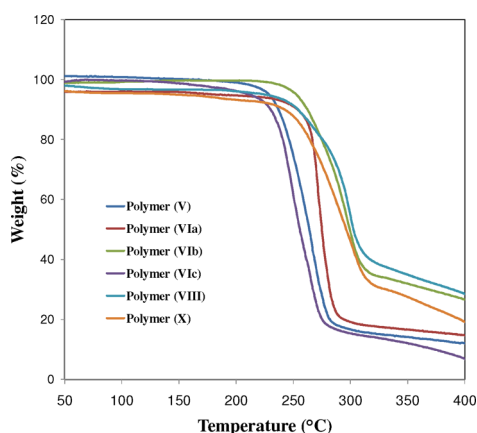


Figure 5. Thermogravimetric analysis (TGA) plots of polymers (V, VIa–c, VIII, and X) with a heating rate of $10\text{ }^{\circ}\text{C min}^{-1}$ under a N_2 atmosphere.

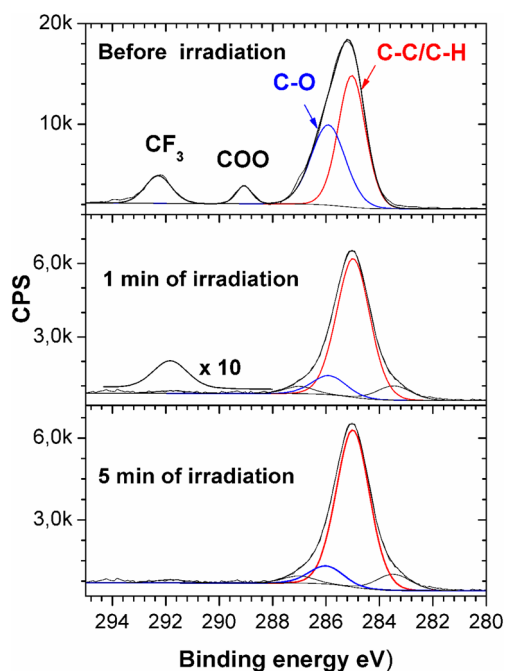


Figure 6. High-resolution XPS spectra of the C 1s envelope of the MAPDST homopolymer films before irradiation and after 1 and 5 min of irradiation via synchrotron radiation (SR) at 103.5 eV .

and the ester groups seemed to be the weakest parts in the MAPDST homopolymer film.

Core-level excitation spectroscopy in its various forms is also a powerful probe of the short-range structure and bonding in molecules and solids. The most prominent spectral features in NEXAFS spectroscopy can be easily monitored during a surface modification treatment. Figure 7 shows that, before MAPDST homopolymer films irradiation, three main signals corresponding to $\text{O } 1s \rightarrow \pi^*_{\text{C=O}}$, $\text{O } 1s \rightarrow \sigma^*_{\text{C-O}}$ and $\text{O } 1s \rightarrow \sigma^*_{\text{C=O}}$ excitations appeared in the NEXAFS spectrum (see Figure 7 top spectrum).^{38,39} The SO_3 contribution of the triflate group can be attributed similar to sulfates and SO_x compounds.^{40,41} The nonstructured spectra have a main absorption peak that can be assigned to the transition from $\text{O } 1s$ to an S-O antibonding orbital at 537.5 eV . This transition is overlapping with the $\text{O } 1s \rightarrow \sigma^*_{\text{C-O}}$ absorption. After irradiation, those features rapidly decreased with an associated change in the

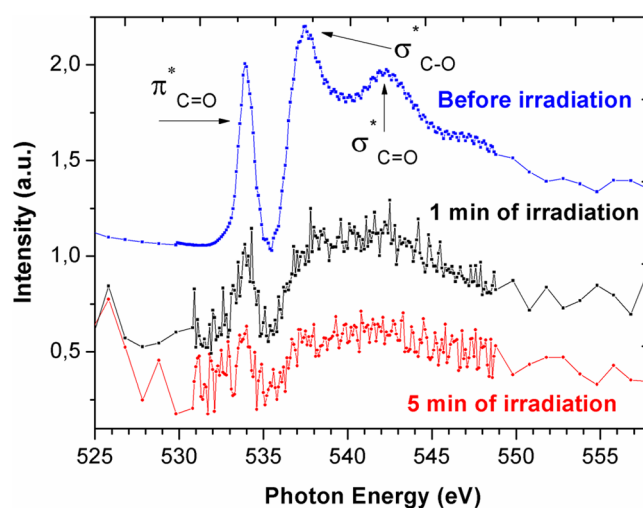


Figure 7. Oxygen K-edge NEXAFS spectra of untreated and SR-irradiated MAPDST homopolymer thin films. Excitation energy = 103.5 eV .

relative intensity, showing evidence that also the SO_3 group together with CF_3 and COO groups are mainly affected by the SR radiation.

The S 2p signals from the (dimethylthio)phenyl and triflate groups are clearly distinguishable, because of the different chemical environment of their S atoms. In particular, the S 2p time evolution with the increase in the irradiation time gives information about the fragmentation process. Figure 8 shows HR-XPS spectra of the S 2p envelope of the MAPDST homopolymer films before irradiation and after SR irradiation. The S 2p core-level spectrum of the pristine MAPDST homopolymer surface shows three spin-orbit split doublets,

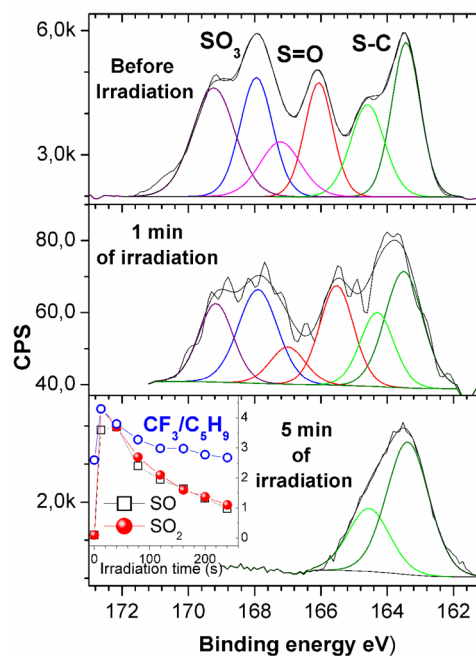


Figure 8. High-resolution XPS spectra of the S 2p envelope of the MAPDST homopolymer films before irradiation and after SR irradiation at 103.5 eV . Inset: Desorption of gases during irradiation of the films at 103.5 eV .

having binding energies that are characteristic of the SO_3 ,⁴² $\text{S}=\text{O}$,⁴² and $\text{S}-\text{C}^{43,44}$ species. After 1 min of irradiation, the XPS signal intensity strongly decreased; after 5 min of irradiation, only the low energy S 2p signal remained. This signal, centered at ~ 163.5 eV (see Figure 8, bottom) shows that, after irradiation, the S–C bonding, probably belonging to the (dimethylthio)phenyl group, resisted the effect of irradiation via SR.

In order to examine the volatile defragmentation products ablated from the irradiated polymer surface, an in situ gas analysis was carried out by QMS simultaneously to the irradiation of the films. The inset of Figure 8 confirms clearly the fragmentation processes discussed in relation to the data presented in Figures 6–8. When the MAPDST homopolymer film is irradiated with SR light, a fast desorption of SO_2^+ , SO^+ , and CF_3^+ fragments ($m/z = 64$, 48, and 69, respectively) was observed. Hydrocarbons were also observed as background gases in the UHV chamber. One of them is the C_5H_9^+ fragment coincident with the CF_3^+ ion. Whereas SO_2^+ and SO^+ intensities increased from zero to reach a maximum and then decreased to zero within a few minutes, the $m/z = 69$ signal increased from a background level to a maximum and then decreased to the original signal before irradiation. The change observed in the intensity of the $m/z = 69$ signal corresponds to the expected desorption of CF_3^+ ions produced by a photon excitation of 103.5 eV.

The conclusions from the EUV irradiation study are given as follows:

- the obtained results showed efficient photodegradation processes that affected mainly the triflate group but also the carbon backbone of the polymers;
- the CH_3SCH_3 group bonded to the phenyl ring was very resistant to the irradiation;
- irradiation at 103.5 eV produced a high rate of gas evolution (SO_2 , SO , and CF_3 fragments); and
- the combination of XPS, NEXAFS, and QMS techniques allowed confirmation of the low stability of the triflate group, compared to the polymer backbone.

Based on the above EUV irradiation data and also that the phenyl C–S bond is stronger than the C– CH_3 bond,⁴⁵ we hypothesized that the neutral sulfide $\text{Ar}-\text{S}-\text{CH}_3$ is formed during the post-exposure bake and development processes. This renders the irradiated area insoluble in the developer, because of the change in polarity from initially hydrophilic to hydrophobic.

Electron Beam Lithography (EBL). As a prelude to EUV lithography (EUVL), extensive EBL of the resists was performed, the details of which are given below.

Resist solutions were prepared by dissolving 3% by weight of the synthesized polymers in methanol solvent. In order to remove particles, all the resist solutions were filtered through a 0.2 μm Teflon filter. The prepared resist solutions of polymers were then spin-coated on 2-in. quarter pieces of *p*-type silicon (100) wafer at 5000 rpm for 60 s to obtain the thin films of polymers. A pre-exposure bake for the resist coated wafers of MAPDST homopolymer (V) and MAPDST-MMA co-polymer (VIa) was performed at 100 °C for 90 s and 90 °C for 90 s, respectively, on a hot plate to remove solvent from the coated resist. Exposures were carried out using EBL (Raith150 system) at the exposure energy of 20 keV with 20 μm aperture and 196.8 pA beam current by covering a broad range of doses. After exposure, a post-exposure bake was performed at 115 °C

for 90 s and 100 °C for 90 s on a hot plate for polymers V and VIa. The exposed samples of polymers V and VIa were developed in 0.003 and 0.022 N tetramethyl ammonium hydroxide (TMAH) solutions prepared in deionized (DI) water by maintaining the solutions at pH 11.5 at room temperature for 17 and 20 s, rinsing them in deionized water for ~ 5 s and ~ 15 s, respectively, and then blow-drying with pure N_2 gas.

The patterning of the synthesized polymeric resists with high resolution was conducted using 20 keV EBL, and the exposed films were developed using an aqueous TMAH developer. Unexposed regions of the resist film readily dissolved in an aqueous TMAH developer while the exposed regions (patterns) were maintained after dipping the exposed resist film in developer. The unexposed polymer was polar in nature, because of the ionic character of the polymer, and, therefore, the unexposed area was readily soluble in water. After exposure to radiation, the polymer loses its ionic character due to degradation of trifluoromethane sulfonate from the sulfonium cation of polymer, as evidenced from the EUV fragmentation studies, and the resulting exposed polymer became less polar, making it insoluble in polar solvents (such as water). The exposed features were evaluated using the scanning electron microscopy (SEM) function that was attached to the Raith 150 system at an energy of 5 keV. HRSEM images of negative tone lines obtained from this polymeric resist were clean and highly resolved. Figure 9 shows the SEM/HRSEM images of

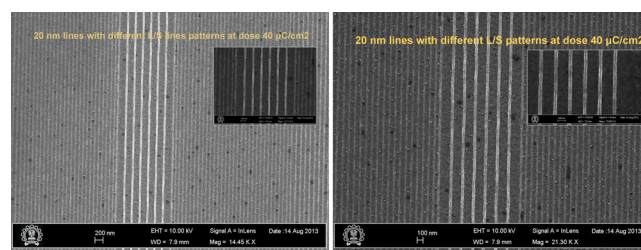


Figure 9. SEM images of the e-beam patterning of negative tone homopolymer (V) and co-polymer (VIa) resists for 20 nm with different line space, exposed at a dose of 40 $\mu\text{C}/\text{cm}^2$ at 20 keV. (Insets show HRSEM images.)

homopolymer (V) and copolymer (VIa) resists upon exposure to an electron beam at 20 keV for 20-nm line patterns with different line/space (exposed at an energy dose of 40 $\mu\text{C}/\text{cm}^2$). The SEM images of EB-exposed resists VIII and X for 20-nm line patterns are provided in the Supporting Information (Figures S4 and S5).

Extreme Ultraviolet Lithography (EUVL). The resist solutions were prepared in methanol and filtered by 0.2 μm Teflon filter and spin-coated onto HMDS-treated 200-mm silicon wafer for ~ 40 nm thin films before EUV exposure evaluation. The resist films of the MAPDST homopolymer (V) and the MAPDST-MMA copolymer (VIa) were prebaked at 100 °C for 90 s and 90 °C for 90 s, respectively. First, test wafers were run to calculate the E_0 center dose value for each of the resist layers. An E_0 center dose of 10 mJ/cm^2 was obtained for the MAPDST-MMA co-polymer and an E_0 center dose of ~ 30 mJ/cm^2 was observed for the MAPDST homopolymer. The resulting photoresist layers were flood exposed with the respective E_0 array using a high-resolution EUV (13.5 nm) lithography tool (SEMATECH Berkeley Microfield Exposure Tool (MET)). Samples were exposed using mask IMO228775 with a field of R4C3. The exposed samples of polymers V and

VIa were post-exposure-baked at 115 °C for 90 s and 100 °C for 90 s, respectively. The exposed samples of polymers V and VIa were developed in a 0.003 N TMAH solution prepared in DI water by maintaining the solution at pH 11.5 at room temperature for 18 s each rinsing in DI water for ~10 s, and then blow-drying with pure N₂ gas to obtain nanofeatures and line space patterns. Figure 10 shows line patterns of the

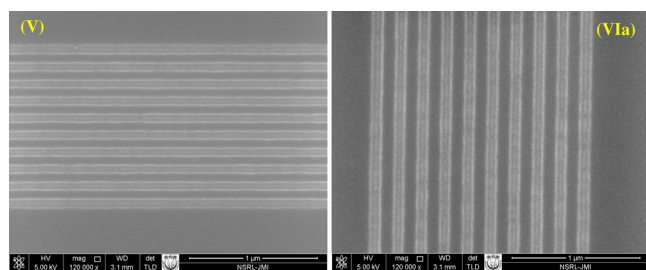


Figure 10. HRSEM images of the EUV patterning of negative tone MAPDST homopolymer resist (V) and poly(MAPDST-co-MMA) resists (VIa) for 20 nm with L/S line/space, respectively.

MAPDST homopolymer (V) and the poly(MAPDST-co-MMA) (VIa) co-polymer resists. The experimental results strongly support our conclusion that these sulfonyl functionalized methyl methacrylate (MMA)-based polymers can be used as potential resist materials for e-beam and EUV lithography.

The EBL studies indicate the capability of our negative tone non-CARs to clearly image at the 20-nm level. Furthermore, from this, we can infer that the inclusion of the dissolution inhibitor (MMA) and the radiation absorption moiety (NVK) increases the photospeed (sensitivity) of the resists, as per the model microstructures previously depicted in Figure 1. This is also carried over to EUVL, where a similar trend is observed. The MAPSDT-MMA copolymer (VIa) has enhanced sensitivity, with respect to the base homopolymer resist.

CONCLUSIONS

Considering the pressing need for highly sensitive photoresist materials in order to meet the requirements of the Semiconductor Industry Roadmap, our efforts were directed to develop different novel polymeric photoresist materials containing the radiation-sensitive sulfonium group. These polymers were synthesized by the polymerization of MAPDST as a common backbone material and methyl methacrylate (MMA) or 4-carboxy styrene (STYCOOH) or *N*-vinyl carbazole (NVK) as a co-unit via a free-radical polymerization process. All these polymers were characterized using instrumental techniques such as Fourier transform-infrared spectroscopy (FT-IR), nuclear magnetic resonance (NMR), gel permeation chromatography (GPC), and thermogravimetric analysis (TGA). As expected, the polymers were found to be sensitive to extreme ultraviolet (EUV) irradiation and the preliminary EUV irradiation experiments at 103.5 eV showed that the triflate and the ester group are the weakest part of the MAPDST homopolymer with important desorption of SO₂⁺, SO⁺ and CF₃⁺ fragments during irradiation. These newly developed polymers were coated on Si wafers and then exposed to electron-beam lithography (EBL) using a 20-keV instrument, while the MAPDST homopolymer (V) and the MAPDST-MMA co-polymer (VIa) were exposed to extreme ultraviolet lithography (EUVL), using a high-resolution (13.5 nm)

lithography tool at different energy doses to obtain 20-nm line patterns with different line/space. Further investigations on high-resolution EBL and EUVL imaging, roughness (line edge roughness (LER) and line width roughness (LWR)), and thickness measurements will be reported in future publications. These 20-nm patterns with the new negative-tone non-chemically amplified resists (non-CARs) developed by us are a significant step up from the chemically amplified resists (CARs) used to achieve features below 20 nm.

ASSOCIATED CONTENT

Supporting Information

Supporting information is included to describe the experimental and lithography procedures, EUV fragmentation and spectral data of the synthesized materials. This material is available free of charge via the Internet at <http://pubs.acs.org>.

AUTHOR INFORMATION

Corresponding Authors

*Tel.: +91 1905237926/+91 1905300065. E-mail: subrata@iitmandi.ac.in (S.G.).

*Tel.: +91 1905237926/+91 1905300065. E-mail: kenneth@iitmandi.ac.in (K.E.G.).

Notes

The authors declare no competing financial interest.

ACKNOWLEDGMENTS

Acknowledgment is made to Intel Corp. USA, for partial support of the project administered by Semiconductor Research Corporation (SRC) USA. IIT Mandi acknowledges the use of the Centre of Excellence in Nanoelectronics (CEN) facilities at IIT Bombay under the Indian Nanoelectronics Users Programme (INUP). This work was also partially supported by the CNPq (process No 550461/2012-4), CAPES, and LNLS, Brazil. The authors would also like to acknowledge the technical assistance of the Accelerator Group, especially the PGM-VUV and Soft X-ray Spectroscopy Group. The use of the Berkeley Microfield Exposure Tool (MET) is also acknowledged.

REFERENCES

- (1) ITRS, *The International Technology Roadmap for Semiconductors*, 2011, available via the Internet at <http://www.itrs.net>.
- (2) Moreau, W. M. *Semiconductor Lithography*; Plenum Publishing Co.: New York, 1988.
- (3) Bloomstein, T. M.; Horn, M. W.; Rothschild, M.; Kunz, R. R.; Palmacci, S. T.; Goodman, R. B. *Lithography with 157 nm lasers*. *J. Vac. Sci. Technol. B* **1997**, *15*, 2112–2116.
- (4) Wong, C. P. *Polymers for Electronic and Photonic Applications*; Academic Press: San Diego, CA, 1993.
- (5) Shaw, J. M.; Seidler, P. F. *Organic electronics: Introduction*. *IBM J. Res. Dev.* **2001**, *45*, 3–9.
- (6) Boutevin, B.; Bosc, D.; Rousseau, A. *Transparent Polymers for Optical Applications*. In *Desk Reference of Functional Polymers: Synthesis and Applications*; Arshady, R., Ed.; American Chemical Society: Washington, DC, 1997; Chapter 3.5, pp 489–503.
- (7) Booth, B. L. *Low loss channel waveguides in polymers*. *J. Lightwave Technol.* **1989**, *7*, 1445–1453.
- (8) Hornak, L. A. *Polymers for Lightwave and Integrated Optics*; Marcel Dekker: New York, 1990.
- (9) Fischbeck, G.; Moosburger, R.; Topper, M.; Petermann, K. *Design concept for single mode polymer waveguides*. *Electron. Lett.* **1996**, *32*, 212–213.

- (10) Lee, H.-J.; Lee, E.-M.; Lee, M.-H.; Oh, M.-C.; Ahn, J.-H.; Han, S. G.; Kim, H. G. Crosslinkable fluorinated poly(arylene ethers) bearing phenyl ethynyl moiety for low loss polymer optical waveguide devices. *J. Polym. Sci., Part A: Polym. Chem.* **1998**, *36*, 2881–2887.
- (11) Boutevin, B.; Rousseau, A.; Bosc, D. New halogenated monomers and polymers for low loss plastic optical fiber. *Fiber Integr. Opt.* **1993**, *13*, 309–319.
- (12) Sarkisov, S.; Teague, Z.; Venkateswarlu, P.; Abdeldagen, H.; Frazier, D.; Adamovsky, G. Formation of a graded-index waveguide in UV exposed polyimide. *J. Appl. Phys.* **1997**, *81*, 2889–2891.
- (13) Watanabe, T.; Ooba, N.; Hayashida, S.; Kurihara, T.; Imamura, S. Polymeric Optical Waveguide Circuits Formed Using Silicone Resin. *J. Lightwave Technol.* **1998**, *16*, 1049–1055.
- (14) Oh, M.-C.; Lee, H.-J.; Lee, M.-H.; Ahn, J.-H.; Han, S. G.; Kim, H. G. Tunable wavelength filters with Bragg gratings in polymer waveguides. *Appl. Phys. Lett.* **1998**, *73*, 2543–2545.
- (15) Eldada, L.; Shacklette, L. W.; Norwood, R. A.; Yardley, J. T. Next-Generation Polymeric Photonic Devices. *Proc. SPIE* **1997**, *CR68*, 207–227.
- (16) Callender, C. L.; Viens, J. F.; Noad, J. P.; Eldada, L. Compact low-cost tunable acrylate polymer arrayed-waveguide grating multiplexer. *Electron. Lett.* **1999**, *35*, 1839–1840.
- (17) Liang, J.; Toussaere, E.; Hierle, R.; Levenson, R.; Zyss, J.; Ochs, A. V.; Rousseau, A.; Boutevin, B. Low loss, low refractive index fluorinated self-crosslinking polymer waveguides for optical applications. *Opt. Mater.* **1998**, *9*, 230–235.
- (18) Kirsten, J. L.; Idriss, B.; James, P. B.; Han, H. C.; Roel, G.; Kevin, S. J.; Ivan, P.; Michael, J. L.; Todd, R. Y.; Andrew, K. W. Chain scission resists for extreme ultraviolet lithography based on high performance polysulfone-containing polymers. *J. Mater. Chem.* **2011**, *21*, 5629–5637.
- (19) Gonsalves, K. E.; Thiagarajan, M.; Choi, J. H.; Zimmerman, P.; Cerrina, F.; Nealey, P.; Golovkina, V.; Wallace, J.; Nikola, B. High performance resist for EUV lithography. *Micron. Eng.* **2005**, *77*, 27–35.
- (20) Gonsalves, K. E.; Wu, H. Preparation of a photoacid generating monomer and its application in lithography. *Adv. Funct. Mater.* **2001**, *11*, 271–276.
- (21) Swaraj, P.; Bengt, R. Methyl Methacrylate (MMA)-Glycidyl Methacrylate (GMA) Copolymers. A novel method to introduce Sulfonic acid groups on the polymeric chains. *Macromolecules* **1976**, *9*, 337–340.
- (22) Mingxing, W.; Wang, Y.; Gonsalves, K. E. New Anionic Photoacid Generator Bound Polymer Resists for EUV Lithography. *Macromolecules* **2007**, *40*, 8220–8224.
- (23) Gonsalves, K. E.; Merhari, L.; Wu, H.; Hu, Y. Organic–Inorganic nanocomposites: Unique resists for nanolithography. *Adv. Mater.* **2001**, *13*, 703–714.
- (24) Gonsalves, K. E.; Wu, H. A novel single-component negative resist for DUV and Electron beam lithography. *Adv. Mater.* **2001**, *13*, 195–197.
- (25) Vipul, J.; Suzanne, M. C.; Jung, J. L.; Matthew, D. C.; Daniel, J. A.; Paul, L.; Maria, E. D.; Nicolas, O.; Su-Jin, K.; Michael, D. W.; Amy, K.; David, A. V.; James, W. T. Impact of Polymerization Process and OOB on Lithographic Performance of a EUV Resist. *Proc. SPIE* **2011**, *7969*, 796912/1–796912/10.
- (26) Thiagarajan, M.; Gonsalves, K. E.; Dean, K.; Sykes, C. H. Design and performance of EUV resist containing photoacid generator for sub-100 nm lithography. *J. Nanosci. Nanotechnol.* **2005**, *5*, 1181–3.
- (27) Wang, M.; Lee, C.-T.; Henderson, C. L.; Yueh, W.; Roberts, J. M.; Gonsalves, K. E. Incorporation of ionic photoacid generator (PAG) and base quencher into the resist polymer main chain for sub-50 nm resolution patterning. *J. Mater. Chem.* **2008**, *18*, 2704–2708.
- (28) Wang, M.; Gonsalves, K. E.; Rabinovich, M.; Yueh, W.; Roberts, J. M. Novel anionic photoacid generators (PAGs) and corresponding PAG bound polymers for sub-50 nm EUV lithography. *J. Mater. Chem.* **2007**, *17*, 1699–1706.
- (29) Itani, T.; Kozawa, T. Resist materials and processes for Extreme Ultraviolet Lithography. *Jpn. J. Appl. Phys.* **2013**, *52*, 1–14.
- (30) Wang, M.; Lee, C. T.; Henderson, C. L.; Yueh, W.; Roberts, J. M.; Gonsalves, K. E. Synthesis and properties of new anionic photoacid generators bound polymer resists for e-beam and EUV lithography. *Proc. SPIE* **2008**, *6923*, 692312.
- (31) Lawson, R. A.; Lee, C. T.; Yueh, W.; Tolbert, L.; Henderson, C. L. Water-developable negative-tone single-molecule resists: High-sensitivity nonchemically amplified resists. *Proc. SPIE* **2008**, *6923*, 692311.
- (32) Shirai, M.; Maki, K.; Okamura, H.; Kaneyama, K.; Itani, T. Non-chemically amplified EUV resist based on PHS. *J. Photopolym. Sci. Technol.* **2009**, *22*, 111–116.
- (33) Skurat, V. Vacuum ultraviolet photochemistry of polymers. *Nucl. Instrum. Methods Phys. Res. B* **2003**, *208*, 27–34.
- (34) Weibel, D. E.; Kessler, F.; da Silva Mota, G. V. Selective surface functionalization of polystyrene by inner-shell monochromatic irradiation and oxygen exposure. *Polym. Chem.* **2010**, *1*, 645–649.
- (35) Lal, J.; Green, R. The preparation of some esters of methacrylic acid. *J. Org. Chem.* **1955**, *20*, 1030–1033.
- (36) Brown, A. A.; Azzaroni, O.; Fidalgo, L. M.; Huck, W. T. S. Polymer brush resist for responsive wettability. *Soft Matter* **2009**, *5*, 2738–2745.
- (37) La, F. B.; Deng, Y.; Kim, R.-H.; Levinson, H. J.; Okoroanyanwu, U.; Sandberg, R.; Wallow, T.; Wood, O. Extreme ultraviolet lithography: From research to manufacturing. *J. Vac. Sci. Technol. B* **2007**, *25*, 2089–2093.
- (38) Klein, R. J.; Fischer, D. A.; Lenhart, J. L. Systematic oxidation of polystyrene by ultraviolet-ozone, characterized by near-edge X-ray absorption fine structure and contact angle. *Langmuir* **2008**, *24*, 8187–8197.
- (39) Outka, D. A.; Stohr, J.; Madix, R. J.; Rotermund, H. H.; Hermsmeier, B.; Solomon, J. NEXAFS studies of complex alcohols and carboxylic acids on the Si(111)(7 × 7) surface. *Surf. Sci.* **1987**, *185*, 53–74.
- (40) Todd, E. C.; Sherman, D. M.; Purton, J. A. Surface oxidation of Chalcocopyrite (CuFeS₂) under ambient atmospheric and aqueous (pH 2–10) conditions: Cu, Fe L- and O K-Edge X-ray spectroscopy. *Geochim. Cosmochim. Acta* **2003**, *67*, 2137–2146.
- (41) Zelenay, V.; Ammann, M.; Krepeloá, A.; Birrer, M.; Tzvetkov, G.; Vernooij, M. G. C.; Raabe, J.; Huthwelker, T. Direct observation of water uptake and release in individual submicrometer sized ammonium sulfate and ammonium sulfate/adipic acid particles using X-ray microspectroscopy. *J. Aerosol Sci.* **2011**, *42*, 38–51.
- (42) Feng, J.; Wen, G.; Huang, W.; Kang, E.-T.; Neoh, K. G. Influence of oxygen plasma treatment on poly(ether Sulphone) films. *Polym. Degrad. Stab.* **2006**, *91*, 12–20.
- (43) Bubnova, O.; Khan, Z. U.; Malti, A.; Braun, S.; Fahlman, M.; Berggren, M.; Crispin, X. Optimization of the thermoelectric figure of merit in the conducting polymer poly(3,4-ethylenedioxythiophene). *Nat. Mater.* **2011**, *10*, 429–433.
- (44) Greczynski, G.; Kugler, T.; Keil, M.; Osikowicz, W.; Fahlman, M.; Salaneck, W. R. Photoelectron spectroscopy of thin films of PEDOT–PSS conjugated polymer blend: A mini-review and some new results. *J. Electron Spectrosc. Relat. Phenom.* **2001**, *121*, 1–17.
- (45) Tsuchida, E.; Shouji, E.; Yamamoto, K. Synthesis of high-molecular-weight poly(phenylene sulfide) by oxidative polymerization via poly(sulfonium cation) from methyl phenyl sulfoxide. *Macromolecules* **1993**, *26*, 7144–7148.